

RESEARCH ARTICLE

# Post Synthesis Functionalization of Graphene Oxide for the Production of Cobalt Nanocomposites in Energy Storage Applications

Jaiby Joseph \*, Mercy Mathews, Arpitha Prabhakaran

**ABSTRACT:** Graphene oxide (GO) and its derivatives have emerged as promising materials for energy storage applications due to their exceptional physical and chemical properties. In this study, nitrogen-doped reduced graphene oxide (N-rGO) and a cobalt-nanocomposite of graphene oxide (Co-N-GO) were synthesized via hydrothermal methods. The structural and compositional characteristics of the resulting materials were confirmed through various analytical techniques, including X-ray diffraction (XRD), Fourier-transform infrared (FTIR) spectroscopy, ultraviolet-visible (UV-Vis) spectroscopy, and Raman spectroscopy. XRD analysis revealed a decrease in the average crystallite size upon nitrogen doping, as determined using the Scherrer equation, indicative of enhanced material dispersion. FTIR spectra provided evidence of successful reduction of GO to rGO and confirmed the presence of C-N bonds, further supporting the doping process. UV-Vis spectroscopy indicated a red shift in absorption peaks towards the visible region, accompanied by a lowering of absorption bands, which suggests the formation of compensating energy states and shifts in conduction band edges due to doping. The bandgap energy, calculated using Tauc plots, showed a significant reduction in N-doped and Co-incorporated samples, highlighting the potential of these materials in enhancing the performance of energy storage devices.

**Keywords:** Graphene Oxide, Doping, Tunable bandgap, Energy storage, N-Graphene.

Received: 30 April 2024; Revised: 21 May 2024; Accepted: 03 June 2024; Available Online: 18 June 2024

## 1. INTRODUCTION

Graphene oxide (GO) and its derivatives have become increasingly significant in the field of material science due to their exceptional physical and chemical properties [1, 2]. Graphene, the parent material, is a two-dimensional carbon material known for its remarkable electrical conductivity, mechanical strength, and thermal stability [3]. However, pristine graphene lacks certain functional groups that are essential for specific applications, particularly in energy storage [4]. Graphene oxide (GO), an oxidized form of graphene, introduces oxygen-containing functional groups such as hydroxyl, carboxyl, and epoxy groups onto its basal plane and edges, thereby enhancing its dispersibility in

solvents and providing sites for further chemical modifications [5]. This functionalization of GO opens avenues for tailoring its electronic, magnetic, and optical properties, making it an ideal candidate for a wide range of applications, including supercapacitors, photodetectors, and fuel cells [6].

Among the various techniques to modify GO, heteroatom doping has emerged as a powerful strategy to enhance its properties further [7]. Doping involves the introduction of foreign atoms into the graphene lattice, thereby altering its electronic structure and chemical reactivity [8]. Nitrogen doping, in particular, has gained attention because nitrogen atoms can easily integrate into the graphene framework due to their comparable atomic size to carbon [9]. When nitrogen atoms replace carbon atoms in the lattice, they introduce localized states near the Fermi level, leading to changes in the band structure. This alteration enables the material to exhibit a reduced bandgap, which is

Kuriakose Elias College Mannanam P.O, Kottayam, India

\* Author to whom correspondence should be addressed:  
[jjoseph@kecollege.ac.in](mailto:jjoseph@kecollege.ac.in) (J. Joseph)

critical for applications that require high electrical conductivity and specific optical properties [10].

The introduction of nitrogen atoms into the graphene lattice not only tunes the bandgap but also enhances the electrochemical performance of graphene oxide [11]. Nitrogen-doped reduced graphene oxide (N-rGO) exhibits higher specific capacitance and better cyclic stability than undoped rGO, making it a promising material for energy storage devices, especially supercapacitors [12]. The nitrogen doping process typically involves post-synthesis treatment of GO with nitrogen-containing precursors, such as ammonia or urea, under thermal or hydrothermal conditions [13]. This process not only incorporates nitrogen into the graphene lattice but also reduces GO, partially restoring the conjugated carbon network, which is crucial for maintaining high electrical conductivity.

In addition to nitrogen doping, the incorporation of transition metal oxides, such as cobalt oxide, into the GO matrix has shown potential for further enhancing the electrochemical and catalytic properties of the material [14, 15]. Cobalt oxide is known for its catalytic efficiency, particularly in oxygen reduction reactions (ORR), which are essential in fuel cell technologies. The combination of nitrogen-doped GO with cobalt oxide leads to the formation of a nanocomposite that benefits from the synergistic effects of both components [16-20]. The cobalt oxide introduces localized magnetic moments, making the composite material suitable for spintronic applications, while the nitrogen doping enhances the overall electrical conductivity and capacitance.

The current study focuses on the post-synthesis functionalization of GO through nitrogen doping and the production of a cobalt nanocomposite (Co-N-rGO) for energy storage applications. The study aims to explore the structural and electronic properties of these materials and assess their potential in enhancing the performance of supercapacitors. By combining nitrogen doping and cobalt oxide incorporation, this research seeks to develop a material with superior electrochemical properties, addressing the growing demand for efficient and high-energy-density storage systems. The findings from this study could pave the way for the development of advanced materials with tailored properties for specific applications in energy storage and beyond. The post-synthesis functionalization of graphene oxide via nitrogen doping and the incorporation of cobalt oxide represents a promising strategy for enhancing the material's properties, making it a valuable candidate for various advanced applications, particularly in the realm of energy storage.

## 2. EXPERIMENTAL DETAILS

### 2.1. Materials and methods

For post synthesis doping of nitrogen and cobalt into rGO, we used a hydrothermal method. rGO was brought from

graphene supermarket. It has 99% purity with 89% C, 9% O and 2% H, 1-10 nm flake thickness and 5-10 micron lateral dimension and 4-8 average number of layers. The purity of rGO was confirmed through XRD analysis. XRD shows a broad peak centered  $2\theta = 26.41^\circ$  characteristic of the 002 plane and it gives an interlayer spacing of 10.3nm according to Scherrer formula.

### 2.2. Preparation of N-rGO

For the preparation of nitrogen doped reduced graphene oxide (N-rGO) hydrothermal method using hydrazine hydrate was used. 0.1 gm of rGO was dispersed in 93ml of deionized water. 7ml of hydrazine hydrate was added to this solution with continuous stirring. After 2h, 5 mL of ammonium hydroxide was added to the mixture with continuous stirring. This mixture was kept in the oven at 180°C for 12 hrs. The residue is collected and washed with deionized water several times to make it pH neutral. The washed residue was then kept in oven at 50°C for 24 h. The resultant powder was collected as N-rGO. This preparation can be repeated with greater doping percentage, say with 9ml of ammonium hydroxide.

### 2.3. Preparation of Cobalt Nanocomposite Co-N-rGO

For the preparation of Co-N-rGO, 10 mg of rGO per mL of water was taken and sonicated for 1h to make it a homogeneous rGO suspension. 8mL of cobalt nitrate hexahydrate  $[\text{Co}(\text{NO}_3)_2 \cdot 6\text{H}_2\text{O}]$  with 10 mM concentration was added drop wise into the rGO suspension with magnetic stirring and sonicated further for 30 minutes. 10 mL of hydrazine hydrate (85%) was also added with a continuous stirring and the mixture was heated at 65°C overnight. The resultant product was cooled, washed and filtered several times with deionized water. The residue is then vacuum dried at 45°C for 24 h and used for further characterization

## 3. RESULTS AND DISCUSSION

In this study, nitrogen-doped reduced graphene oxide (N-rGO) and cobalt nanocomposite nitrogen-doped graphene oxide (Co-N-rGO) were synthesized and characterized using a combination of Raman spectroscopy, Fourier-transform infrared spectroscopy (FTIR), X-ray diffraction (XRD), and UV-visible spectroscopy. The detailed results and their implications for the structural, chemical, and optical properties of the synthesized materials are discussed below.

### 3.1. Raman-scattering analysis

Raman spectroscopy was employed to investigate the structural changes induced by nitrogen doping and cobalt

nanocomposite formation in reduced graphene oxide (rGO). Raman spectroscopy is a powerful tool for characterizing carbon-based materials, as it provides insight into the degree of disorder and defect density within the graphene lattice.

### 3.1.1. Raman Spectra of N-rGO

The Raman spectra of rGO and N-rGO are presented in Figure 1. The characteristic peaks associated with graphene-based materials are observed at  $1342\text{ cm}^{-1}$  and  $1559\text{ cm}^{-1}$ , corresponding to the D band and G band, respectively. The D band is associated with the presence of in-plane and edge defects within the graphene lattice, while the G band represents the in-plane vibrations of  $\text{sp}^2$ -bonded carbon atoms [21].

In the case of N-rGO, the Raman spectra reveal an increase in the intensity of the D band relative to the G band, which is indicative of the introduction of defects due to nitrogen doping. The degree of disorder introduced by nitrogen atoms is quantitatively evaluated by the ID/IG ratio, where ID and IG are the intensities of the D and G bands, respectively. For rGO, the ID/IG ratio is calculated to be 0.49, while for N-rGO, this ratio increases to 0.73. The increase in the ID/IG ratio confirms that nitrogen doping introduces additional defects into the graphene lattice, likely due to the incorporation of nitrogen atoms into the carbon framework, creating disordered regions and altering the electronic structure of the material. These defects are beneficial for enhancing the electrochemical activity and catalytic properties of the material, making N-rGO a promising candidate for energy storage applications.

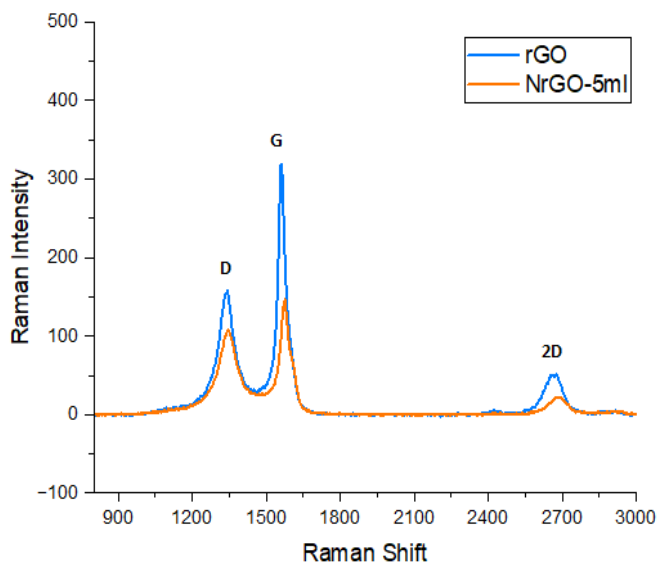


**Fig. 1.** Raman spectra of rGO and N-doped rGO.

### 3.1.2. Raman Spectra of Co-N-rGO

Figure 2 presents the Raman spectra of rGO and Co-N-rGO.

In Co-N-rGO, the D and G bands are observed at  $1351.98\text{ cm}^{-1}$  and  $1575.10\text{ cm}^{-1}$ , respectively. Similar to N-rGO, the introduction of cobalt into the nitrogen-doped graphene oxide matrix leads to an increase in the intensity of the D band. The ID/IG ratio for Co-N-rGO is significantly higher at 1.06, compared to 0.49 for rGO and 0.73 for N-rGO. This substantial increase in the ID/IG ratio suggests a higher density of defects in Co-N-rGO compared to N-rGO.

The higher defect density in Co-N-rGO can be attributed to the formation of cobalt nanocomposites on the surface of N-rGO. The cobalt atoms likely create additional disorder within the graphene lattice, further enhancing the material's defect sites. These defects are crucial for improving the material's catalytic activity, as they provide more active sites for electrochemical reactions, which is particularly advantageous for applications such as oxygen reduction reactions (ORR) in fuel cells and supercapacitors.

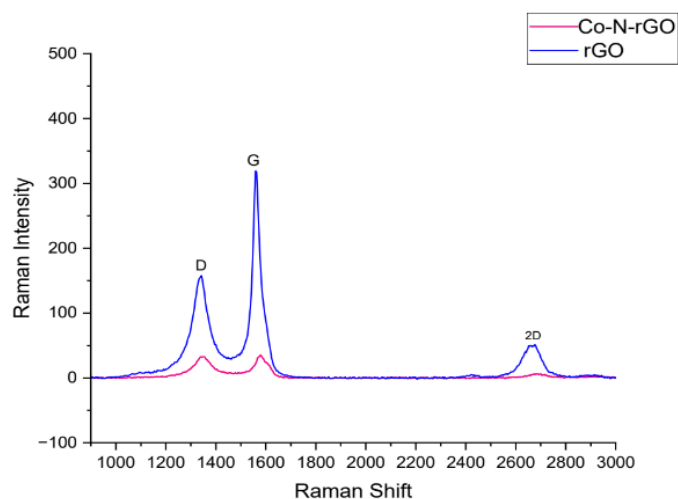


**Fig. 2.** Raman spectra of rGO and Co incorporated N-rGO.

## 3.2. FTIR analysis

Figure 3 presents the Fourier-transform infrared (FTIR) spectra of rGO, N-rGO, and Co-N-rGO samples, which provide valuable insights into the chemical bonding and functional groups present in these materials. FTIR spectroscopy is instrumental in identifying various functional groups and confirming the successful doping of nitrogen and incorporation of cobalt into the graphene oxide matrix. In the FTIR spectrum of rGO, a characteristic dip is observed at around  $1200\text{ cm}^{-1}$ , which corresponds to the stretching vibration of  $\text{C}=\text{C}$  bonds within the graphene lattice. This indicates the presence of conjugated double bonds, which are typical of the  $\text{sp}^2$  hybridized carbon network in graphene-based materials [22].

Upon nitrogen doping (N-rGO), a new and prominent dip appears at approximately  $1187\text{ cm}^{-1}$ , which is indicative of the C-N bond formation. This shift in the transmittance curve confirms the successful incorporation of nitrogen atoms into the rGO structure. The C-N bond is crucial for enhancing the material's electronic properties, as nitrogen doping

introduces new electronic states within the band structure of graphene, thereby modifying its conductivity and chemical reactivity. Similarly, the FTIR spectrum of Co-N-rGO also displays a strong dip at around  $1187\text{ cm}^{-1}$ , corresponding to the C-N bond. The presence of this dip in both N-rGO and Co-N-rGO suggests that the nitrogen doping process was consistent and effective in introducing nitrogen into the graphene oxide lattice [23]. Additionally, the reduction process of rGO during synthesis is evidenced by the disappearance or weakening of oxygen-containing functional groups, further confirming the reduction of GO and successful doping of nitrogen. The incorporation of cobalt, while not directly observable in the FTIR spectrum due to overlapping peaks, is inferred through the structural changes and chemical bonding observed in the spectra.

### 3.3. X-ray diffraction analysis

X-ray diffraction (XRD) analysis was performed to determine the crystalline structure and phase composition of the synthesized rGO and Co-N-rGO samples. XRD is a powerful technique that provides information about the interlayer spacing, crystallite size, and the degree of exfoliation in graphene-based materials. Figure 4 shows the XRD patterns of rGO and Co-N-rGO. The characteristic peak of graphite, corresponding to the 002 plane, is observed at a

$2\theta$  angle of  $26.5^\circ$  (JCPDS #656212). In the case of rGO, a similar peak appears at  $2\theta = 26.4^\circ$ , with an interplanar spacing (d) value of  $0.337\text{ nm}$ . This peak represents the ordered stacking of graphene layers in the rGO structure [24].

For Co-N-rGO, the XRD pattern also exhibits a humped peak at  $2\theta = 26.30^\circ$ , with an interplanar spacing of  $0.338\text{ nm}$ . This slight shift in the peak position, compared to rGO, suggests that the introduction of cobalt and nitrogen into the graphene oxide matrix has caused minor structural changes, likely due to lattice distortion and strain. The crystallite size (L) was calculated using the Scherrer equation, and it was found to be  $10.27\text{ nm}$  for rGO and  $7.84\text{ nm}$  for Co-N-rGO. The decrease in crystallite size for Co-N-rGO indicates that cobalt and nitrogen incorporation leads to a more fragmented or disordered structure, which is consistent with the observations from Raman spectroscopy [24].

The average number of graphene layers (N) was also calculated using the equation:

$$N = (L/d) + 1$$

For rGO, the number of layers was determined to be 31.4, while for Co-N-rGO, it decreased to 24.2. The reduction in the number of layers further corroborates the exfoliation and structural changes induced by cobalt and nitrogen doping.

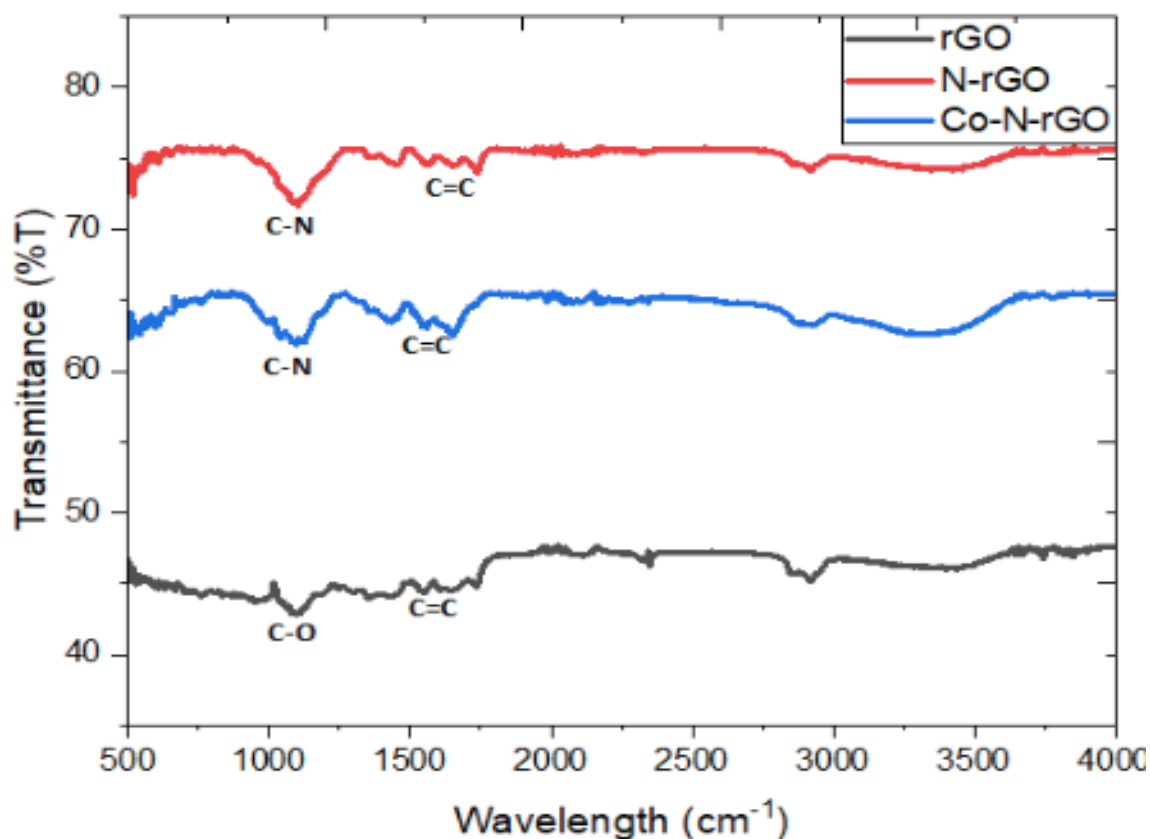


**Fig. 3.** FTIR Spectra of rGO, N-rGO and Co-N-rGO.



The XRD pattern of Co-N-rGO shows broader peaks compared to rGO, particularly the peak corresponding to the 002 plane. Peak broadening in XRD patterns can be attributed to several factors, including instrumental effects, reduced crystallite size, and lattice strain. In the case of Co-N-rGO, the broader peak is likely due to the smaller crystallite size and the strain induced by cobalt incorporation and nitrogen doping. The presence of cobalt on the surface of N-doped rGO creates localized lattice strain, leading to further peak broadening. Moreover, the broadening of the 002 plane peak in Co-N-rGO suggests a reduction in crystallinity, which is often associated with increased defect density and disordered stacking of graphene layers. Despite this reduction in crystallinity, the level of exfoliation observed in Co-N-rGO is comparable to that of rGO, indicating that cobalt impregnation and nitrogen doping do not significantly compromise the material's exfoliation. It is important to note that most of the characteristic peaks of cobalt or cobalt oxide overlap with the GO peaks in the XRD pattern, making it challenging to distinctly identify cobalt phases. However, the structural changes observed in the XRD pattern provide indirect evidence of cobalt incorporation and its impact on the material's crystalline structure.

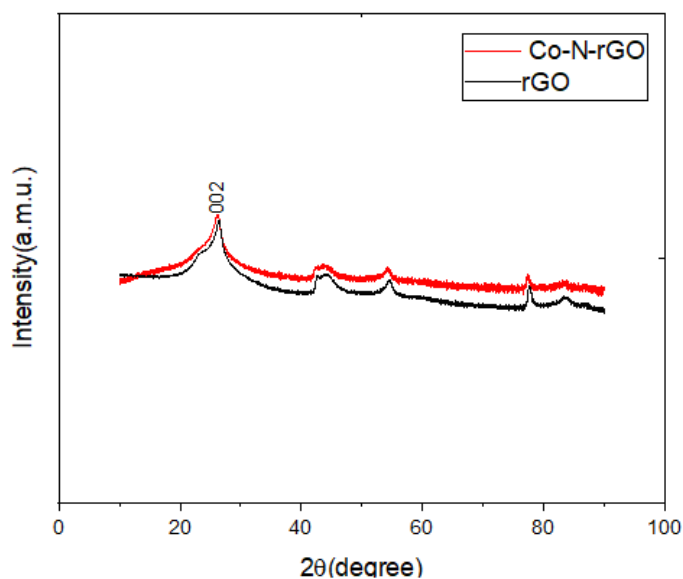


**Fig. 4.** X-ray Diffraction Pattern of rGO and Co-N-rGO.

### 3.4. UV-Visible spectroscopy analysis

UV-visible spectroscopy is a powerful technique for understanding the optical properties of materials, particularly in determining the absorption characteristics and energy band gaps of reduced graphene oxide (rGO) and its derivatives. In this study, UV-visible spectroscopy was employed to analyze rGO, N-rGO, and Co-N-rGO to reveal their band gaps and absorption behavior.

The UV-visible spectra of rGO and N-rGO provide crucial insights into their electronic structure and the effects

of nitrogen doping. Figure 5 illustrates the Tauc plot for both rGO (left) and N-rGO (right), with the corresponding absorption spectra shown in the insets. The absence of a distinct absorption band at around 300 nm in the rGO sample indicates the successful elimination of oxygen-containing functional groups during the reduction process. The reduction of graphene oxide (GO) typically leads to the restoration of the  $sp^2$  hybridized carbon network, resulting in a significant decrease in oxygen content and an increase in electrical conductivity.

Upon nitrogen doping, the N-rGO sample exhibits a new absorption peak in the range of 316-330 nm. This peak is indicative of the further reduction of GO and the consequent restoration of the  $\pi$ -conjugation network due to the presence of nitrogen atoms. The introduction of nitrogen into the graphene lattice is known to alter the electronic structure by introducing new energy states, which can modify the optical properties and enhance the material's electrochemical performance. The appearance of this peak in the UV-visible spectrum of N-rGO suggests that nitrogen doping not only reduces the bandgap but also facilitates the restoration of the conjugated system, making the material more conductive and suitable for various applications, such as energy storage and catalysis.

The energy band gaps of rGO and N-rGO were evaluated using the Tauc plot method, which is based on the Tauc relation:

$$(\alpha h\nu)^2 = A(h\nu - E_g)$$

where  $h\nu$  represents the photon energy,  $A$  is a constant, and  $\alpha$  is the linear absorption coefficient. The Tauc plot is constructed by plotting  $(\alpha h\nu)^2$  against  $h\nu$ , and the x-intercept of the extrapolated linear portion of the curve provides the bandgap  $E_g$  of the material.

For rGO, the Tauc plot reveals a bandgap in the range of 2.5 to 3.7 eV. The variation in the bandgap can be attributed to the uneven oxidation of GO sheets during the reduction process. The presence of residual oxygen functional groups and defects within the rGO structure contributes to the broad range of bandgap values. This variability in the bandgap is a common feature of rGO, as the degree of reduction and the extent of defect healing can vary between samples, leading to different electronic properties.

In contrast, the Tauc plot for N-rGO shows a reduced bandgap in the range of 1.6 to 2.8 eV. The decrease in the bandgap upon nitrogen doping is a significant finding, as it indicates that the introduction of nitrogen atoms into the graphene lattice effectively narrows the bandgap. This tunability of the bandgap is particularly important for optimizing the electrochemical activity of rGO-based materials. A lower bandgap enhances the material's conductivity and electron mobility, making N-rGO a promising candidate for applications in supercapacitors, batteries, and other electronic devices.

The UV-visible spectrum and Tauc plot of Co-N-rGO are shown in Figure 6. The absorption spectrum of Co-N-rGO exhibits a peak at around 230 nm, which is characteristic of the retained rGO components, albeit with reduced intensity.

This peak suggests that the fundamental structure of rGO is preserved even after cobalt incorporation, but with some modifications due to the introduction of cobalt and nitrogen.

Additionally, a smaller peak appears in the absorption band around 327-380 nm in the Co-N-rGO sample. This peak can be attributed to the interaction between cobalt atoms and the nitrogen-doped graphene lattice. The introduction of cobalt into the N-rGO matrix leads to further modifications in the electronic structure, likely due to the formation of Co-N bonds or the creation of new defect states within the graphene lattice. These changes are reflected in the optical properties of Co-N-rGO, as evidenced by the appearance of

the new absorption peak.

The Tauc plot of Co-N-rGO reveals a bandgap in the range of 1.6 to 3.5 eV. This tunable bandgap is a key feature of Co-N-rGO, as it allows for the adjustment of the material's electronic properties to suit specific applications. The wider range of bandgap values in Co-N-rGO, compared to N-rGO, suggests that cobalt incorporation introduces additional complexity into the material's electronic structure. This complexity could arise from the formation of cobalt-related defect states or from the interaction between cobalt and nitrogen within the graphene lattice [24].

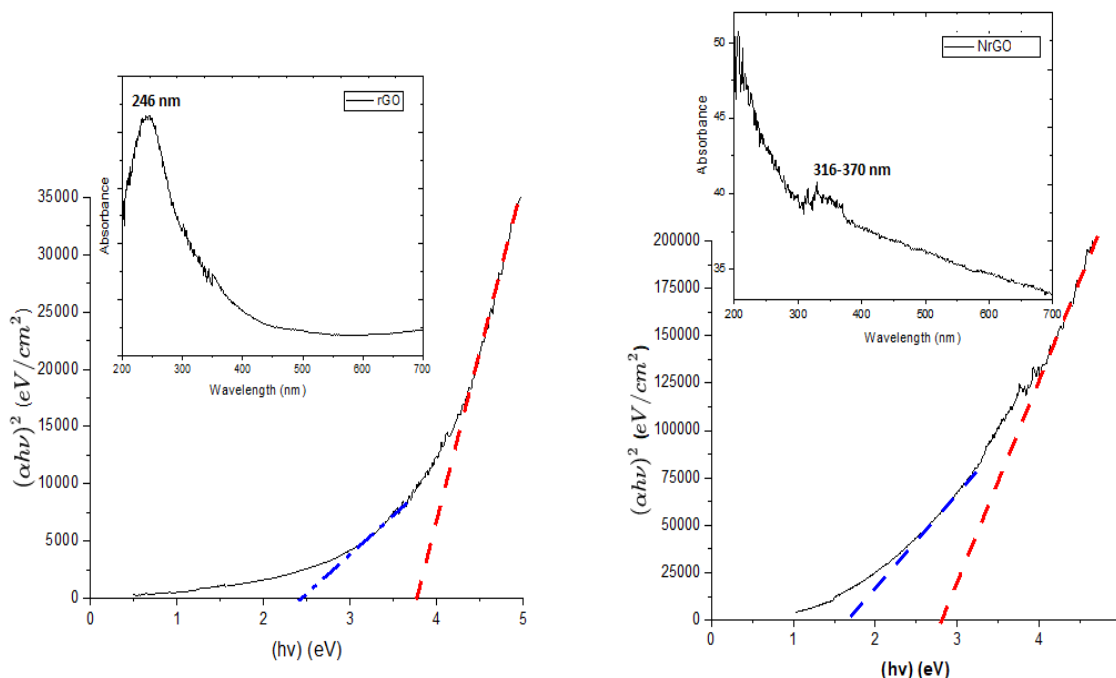


Fig. 5. The Tauc plot and absorption band of rGO (left), N-rGO (right).

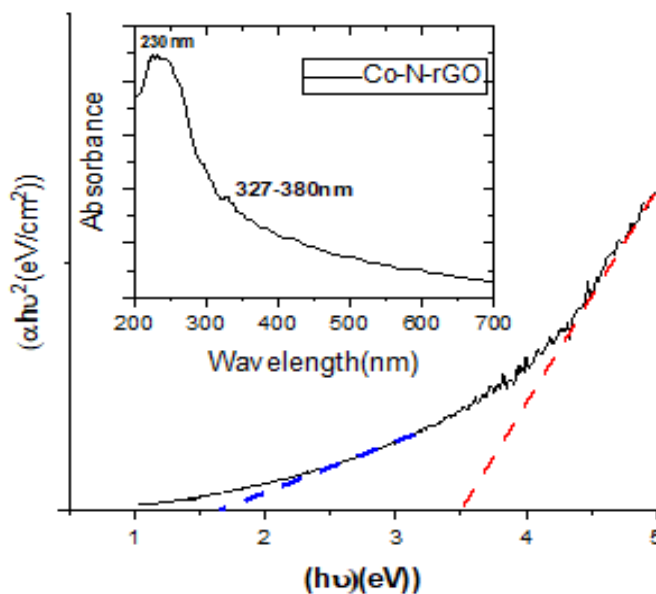


Fig. 6. The Tauc plot and absorption band of Co-N-rGO.

## 4. CONCLUSION

A straightforward hydrothermal method was employed to synthesize nitrogen-doped graphene (N-rGO) using ammonium hydroxide as the nitrogen source. Additionally, a cobalt-incorporated, nitrogen-doped graphene nanocomposite (Co-N-rGO) was successfully synthesized through a single-step process, which simultaneously achieved the reduction of graphene oxide (GO) and nitrogen doping. Characterization techniques such as XRD, Raman, and FTIR spectroscopy confirmed the successful doping of rGO with nitrogen (N-rGO) and the formation of the cobalt nanocomposite (Co-N-rGO). The optical properties of the synthesized samples were analyzed using UV-visible spectroscopy, revealing a shift in the absorption region from the UV to the visible range for both N-rGO and Co-N-rGO. This shift is accompanied by a reduction in bandgap, demonstrating the tunability of the bandgap with appropriate doping. This economical and efficient method offers a promising approach for the mass production of these materials. The unique properties exhibited by N-rGO, including its tunable bandgap, make it a highly promising electrode material for energy storage applications. Moreover, the cobalt nanocomposite has proven to be an effective catalyst for oxygen reduction reactions (ORR) in fuel cells, highlighting its potential for use in advanced energy technologies.

## CONFLICT OF INTEREST

The authors declare that there is no conflict of interests.

## REFERENCES

- [1] Farooq, N., Rehman, Z., Hareem, A., Masood, R., Ashfaq, R., Fatimah, I. Hussain, S., Ansari, S. A. and Parveen, N. **2024**. Graphene oxide and based materials: Synthesis, properties, and applications- A comprehensive review. *MatSci Express* 1(4), pp. 185-231.
- [2] Borane, N., Boddula, R., Odedara, N., Singh, J., Andhe, M. and Patel, R., **2024**. Comprehensive review on synthetic methods and functionalization of graphene oxide: Emerging Applications. *Nano-Structures & Nano-Objects*, 39, p.101282.
- [3] Yoshikawa, T., Mabuchi, Y., Terauchi, S., Yamada, N., Okuda, S. and Araki, S., **2024**. Effect of dispersing graphene oxide with different specifications in water on lubrication performance. *Tribology International*, p.109886.
- [4] Endogdu, G. **2024**. Voltammetric detection of diazinon insecticide at ferrocene-graphene/nafion modified glassy carbon electrode. *ChenSci Advances* 1(2), pp. 104-110.
- [5] Tchekep, A.K., Suryanarayanan, V. and Pattanayak, D.K., **2024**. Simultaneous synthesis of sulfonated reduced graphene oxide@ graphene oxide hybrid material for efficient electrochemical sensing of silver ions in drinking water. *Carbon Trends*, p.100393.
- [6] Cavusoglu, H., Ibrahim, M.A., Sakalak, H., Günes, E., Uysal, A., Çıtak, E. and Öztürk, T., **2024**. Graphene Oxide Boosted: A Multifaceted Examination of CZTS Composite for Enhanced Photocatalysis and Antimicrobial Efficacy. *Journal of Nanoelectronics and Optoelectronics*, 19(7), pp.700-711.
- [7] Anand, S., Yadav, R. K., Yadav, A. N., Singh, S., Shahin, R., Baeg, J. O., Singh, K., Pandey, M., Yadav, S. and Dwivedi, D.K. **2024**. Unlocking the power of solar synergy: Enhanced nitrophenol degradation using ADGCAAQ photocatalyst. *ChemSci Advances* 1(2), pp. 77-87.
- [8] Kumar, M.P., Kesavan, T., Kalita, G., Ragupathy, P., Narayanan, T.N. and Pattanayak, D.K., **2014**. On the large capacitance of nitrogen doped graphene derived by a facile route. *RSC Advances*, 4(73), pp.38689-38697.
- [9] Li, C., Wang, X., Liu, G., Guo, Z., Zhao, B., Liang, J., Umar, A., Hao, H. and Li, W., **2023**. Three-dimensional architecture of sulfur doped graphene for supercapacitor. *Journal of Nanoelectronics and Optoelectronics*, 18(6), pp.647-651.
- [10] Kottakkat, T. and Bron, M., **2014**. One-Pot Synthesis of Cobalt-Incorporated Nitrogen-Doped Reduced Graphene Oxide as an Oxygen Reduction Reaction Catalyst in Alkaline Medium. *ChemElectroChem*, 1(12), pp.2163-2171.
- [11] Abdullah, M.M., Nizam, R., Albargi, H.B., Ahmad, M.Z., Ahmad, J., Khan, M. and Mustafa, J., **2023**. Power Spectrum of Dual Varieties of Graphene Allotropes. *Journal of Nanoelectronics and Optoelectronics*, 18(2), pp.160-167.
- [12] Bondareva, J.V., Logunov, M.A., Dyakonov, P.V., Rubekina, A.A., Shirshin, E.A., Sybachin, A.V., Maslakov, K.I., Kirsanova, M.A., Osipenko, S.V., Kvashnin, D.G. and Sukhanova, E.V., **2024**. Tracking the quality of graphene oxide suspension during long-term storage. *Surfaces and Interfaces*, 52, p.104842.
- [13] Hu, L., Abou Zeid, S., Bistintzanos, A., Khaoulani, S., Drago, D., Ghasemi, R., Muller, F., Gervais, M., Sollogoub, C., Goldmann, M. and Remita, S., **2024**. One-pot radiolytically synthesized reduced graphene

- oxide-gold nanoparticles composites and exploration in energy storage. *Applied Surface Science*, p.161109.
- [14] Ike, S.N. and Vander Wal, R., **2024**. Templating-induced graphitization of novolac using graphene oxide additives. *Carbon Trends*, *16*, p.100388.
- [15] Olea, M.A.U., Bueno, J.D.J.P., Real, J.A.D., Suárez, A.A.M., Robles, J.F.P., Pérez, A.X.M. and Largo, S.Y., **2024**. Self-assembled graphene oxide thin films deposited by atmospheric pressure plasma and their hydrogen thermal reduction. *Materials Letters*, *363*, p.136334.
- [16] de França, J.A.A., Navarro-Vázquez, A. and Hallwass, F., **2024**. Synthesis and characterization of grafted graphene oxide materials with lyotropic liquid crystalline properties detected by NMR spectroscopy. *Materials Letters*, *366*, p.136526.
- [17] Mitiushhev, N.D., Khodos, I.I., Kabachkov, E.N., Shatalova, T.B., Panin, G.N. and Baranov, A.N., **2024**. Chemical stitching of a reduced and fluorine decorated graphene oxide quilt. *Materials Letters*, *372*, p.136989.
- [18] Azloulk, M., Kabatas, M.A.B.M., Eker, Y.R., Zor, E. and Bingol, H., **2024**. Graphene oxide nanocellulose composite as a highly efficient substrate-free room temperature gas sensor. *Results in Engineering*, *22*, p.102228.
- [19] Thakran, M., Shukla, S., Brajpuriya, R. and Kumar, B., **2024**. Amplified adsorption and photocatalytic degradation of polycyclic aromatic hydrocarbons using biocompatible nanocrystalline reduced graphene oxide quantum dots. *Journal of Photochemistry and Photobiology A: Chemistry*, p.115798.
- [20] Fan, J., Li, D. and Wang, X., **2016**. Effect of modified graphene quantum dots on photocatalytic degradation property. *Diamond and Related Materials*, *69*, pp.81-85.
- [21] Ruby Kamalam, M.B., Inbanathan, S.S.R., Mustafa, J., Abdullah, M.M., Husain, S. and Sethuraman, K., **2024**. A Comparative Study on the Degradation of Methylene Blue and Methyl Orange Dyes Under the Irradiation of Visible Light Using GO–CdO Nanocomposites. *Journal of Nanoelectronics and Optoelectronics*, *19*(6), pp.634-645.
- [22] Kimiagar, S. and Abrinaei, F., **2018**. Third-order optical nonlinearity of N-doped graphene oxide nanocomposites at different GO ratios. *Optical Materials*, *79*, pp.120-128.
- [23] Abrinaei, F., Kimiagar, S. and Gharedaghi, S., **2018**. Strong optical nonlinearity of CdS/nitrogen-doped reduced graphene oxide nanocomposites using Z-scan technique. *Journal of Materials Science: Materials in Electronics*, *29*, pp.2550-2560.
- [24] Karteri, I., Karataş, Ş., Çavaş, M., Arif, B. and Yakuphanoglu, F., **2016**. The dielectric and optoelectronic properties of graphene oxide films by solution-casting technique. *Journal of Nanoelectronics and Optoelectronics*, *11*(1), pp.29-35.